Development of quantitative detection method for mass spectrometry coupled to an infrared laser spectroscope (Picarro) to monitor in nitrogen matrix a complex gas mixture of H2, He, CO, N2, Ne, O2, Ar, CO2, H2S, CH4, C2H4, C2H6, C3H6, C3H8, i-C4H10, n-C4H10, and C5H12

Seny Keita, Sonia Noirez, Guillaume Berthe, Agnes Vinsot, Byeong Seok Kim, Matthieu Mascle, Mélanie Lundy, Bruno Garcia

Received: 18 April 2023 | Revised: 7 July 2023 | Accepted: 10 July 2023

DOI: 10.1002/rcm.9614

RESEARCH ARTICLE

Rapid Communications in Mass Spectrometry WILEY

Development of quantitative detection method for mass spectrometry coupled to an infrared laser spectroscope (Picarro) to monitor in nitrogen matrix a complex gas mixture of H_2, He, CO, N_2, Ne, O_2, Ar, CO_2, H_2S, CH_4, C_2H_4, C_2H_6, C_3H_6, C_3H_8, *i*-C_4H_{10}, *n*-C_4H_{10}, and C_5H_{12}

Seny Keita[1,2,3] | Sonia Noirez[2] | Guillaume Berthe[2] | Agnes Vinsot[3] | Byeong Seok Kim[2] | Matthieu Mascle[2] | Mélanie Lundy[3] | Bruno Garcia[2]

[1]Géosciences, Ressources Naturelles et Environnement (GRNE), Sorbonne Université Faculté des Sciences et Ingénierie, Paris, France

[2]IFP Energies nouvelles, Rueil-Malmaison, France

[3]Andra, Laboratoire de Recherche Souterrain de Meuse/Haute-Marne, Bure, France

Correspondence
S. Keita, Géosciences, Ressources Naturelles et Environnement (GRNE), Sorbonne Université Faculté des Sciences et Ingénierie, 4 Pl. Jussieu, Paris, Île-de-France 75005, France.
Email: seny3keita@gmail.com; seny.keita@ifpen.fr

Funding information
IFP Energies Nouvelles; Agence Nationale pour la Gestion des Déchets Radioactifs

Rationale: The deep geological repository is considered the international reference for radioactive waste management. All gas exchanges must be understood in the context of the feasibility of such a repository. The technological challenge is to continuously monitor a wide range of gaseous molecules at low concentrations in confined spaces.

Methods: A gas monitoring station, composed of two complementary analyzers, was developed: an electron impact quadrupole mass spectrometer (HPR-20 R&D Hiden Analytical) and an infrared laser spectroscope (Picarro). The spectrometer was calibrated using simple mixtures (i.e., C_2H_6 in N_2) and multiple mixtures (i.e., H_2, He, CO_2, CH_4, and O_2 in N_2) at different concentrations to correct interferences. A matrix calculation is proposed to calculate the relative concentrations.

Results: The method developed allows the measurement of gaseous species: light hydrocarbons, noble gases, sulfides, greenhouse gases, oxygen, hydrogen, and nitrogen in the same mixture. For each gas, the SDs and the limits of detection and quantification were calculated. The method was validated by comparing the concentrations of the measured gas species with the reference values of two standard gas cylinders.

Conclusions: Calibration of a complex gas mixture remains a challenge because fragmentation of molecules, especially hydrocarbons, reduces the sensitivity of the method. The method developed is suitable for continuous gas monitoring in a confined environment and can be implemented to perform experiments in underground structures: galleries, microtunnels (cells), and boreholes.

1 | INTRODUCTION

Clay-rich rocks are considered to host high-level and intermediate-level, long-lived radioactive waste geological repositories. Therefore, in recent decades, the study of water–gas–rock interactions in clay-rich rocks has benefited from the creation of underground research laboratories (URL) in this type of environment in Belgium and Switzerland as well as in France.[1] These URLs facilitate simultaneous

access to two or even three phases (water, gas, and rock) during in situ experiments. Andra's Meuse/Haute-Marne URL galleries (−490 m depth) are ventilated with outdoor air from the surface. This air interacts with all the surfaces of the rock (Callovo-Oxfordian clay) it encounters (Figure 1A) and with the laboratory building materials such as concrete and steel. It becomes enriched with water vapor coming from the rock and other gases present in a dissolved state in the rock pore water (like N_2, light alkanes and alkenes, and CO_2). On the one hand, oxygen from the air is consumed by the reaction mainly with pyrites and organic matter present in the rock.[1] On the other hand, if there is no oxygen, anoxic corrosion of the steel in the structures can occur in the presence of water. This corrosion generates hydrogen.[2]

To understand these interactions and to evaluate the chemical evolution inside the underground structures (boreholes, microtunnels, and galleries) over time, a major effort has been made to develop a wide range of methods and instruments adapted to URL conditions around the world.[1–9] Such methods and instruments include gas chromatography (micro GC),[1,3] infrared (IR) spectrometry,[6–8] Raman spectroscopy,[8,9] Fourier-transform infrared spectroscopy (FTIR),[6] and mass spectrometry (MS).[4,5] The advantage of GC is that it can provide a quantitative analysis of complex gas mixtures, whereas its main disadvantage is that it does not measure a wide range of carbon species.[10,11] Conventional absorption techniques such as FTIR and IR spectrometry fail to meet certain requirements in terms of sensitivity and selectivity.[12] Raman spectroscopy is nondestructive and enables

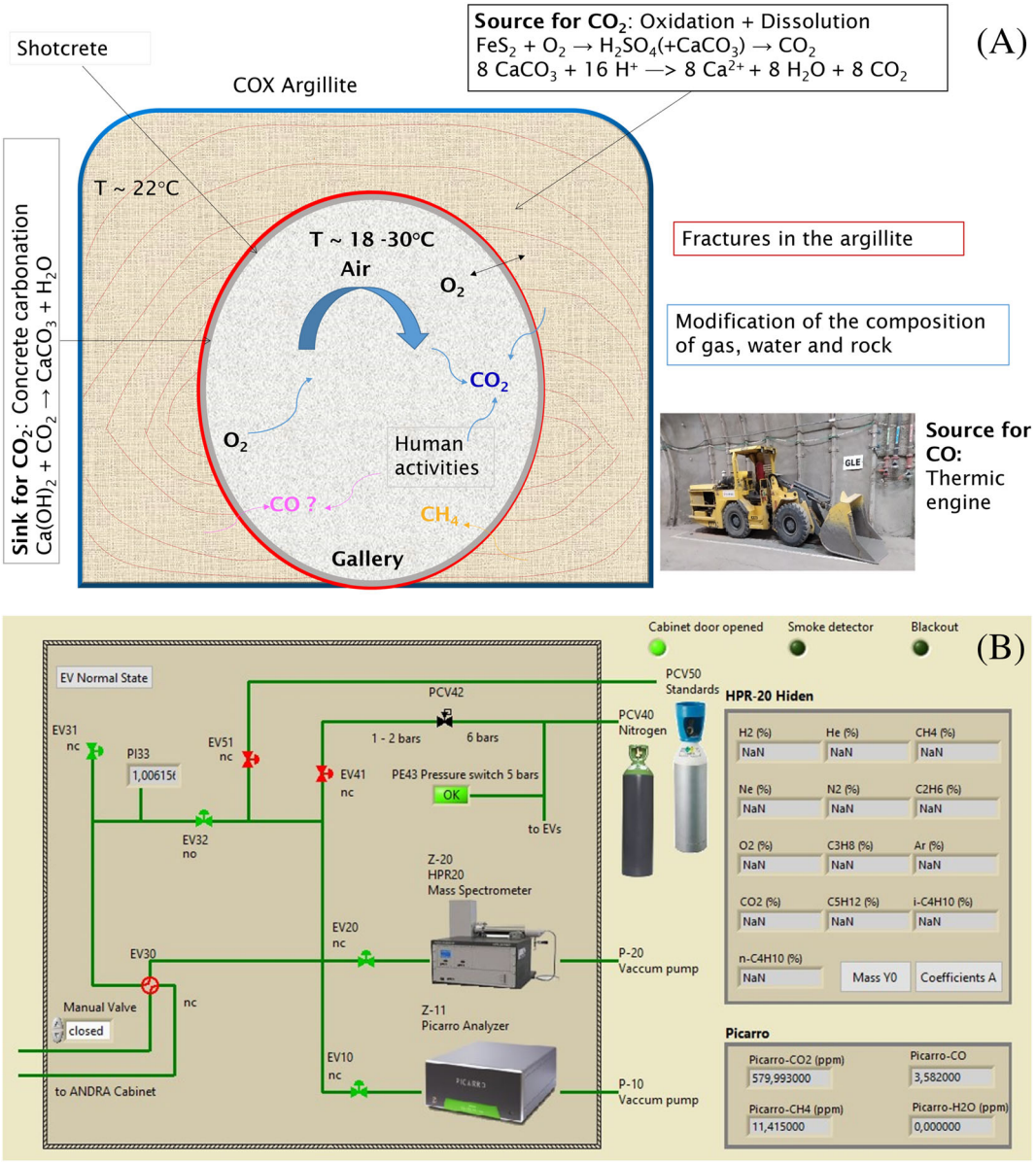

FIGURE 1 A, Summary scheme of the main mechanisms and gas exchanges occurring in a gallery of the Meuse/Haute-Marne URL. B, Schematic diagram from screen control of Flair Soil used for mass spectrometer calibration and online monitoring of gas composition [Color figure can be viewed at wileyonlinelibrary.com]

the detection of homonuclear diatomic gases (e.g., H_2, N_2, and O_2), which are not active in the IR spectrometry. Like IR spectrometry, Raman spectroscopy has low sensitivity. The wavelength-scanned cavity ring-down spectroscopy (WS-CRDS) (Picarro)[13] has been developed to meet the challenges of sensitivity and selectivity. The WS-CRDS technology offers advantages over traditional IR and FTIR-based analyzers. It features high sensitivity, due to a longer light path trapped in a very thin optical cavity. However, its spectral range is limited, and the results depend on the gas matrix used.[14]

In URL, nonoptical techniques such as MS[4,5] and GC[1,3,7,8] are used for measuring the partial pressures of CO_2, H_2, CH_4, N_2, O_2, and noble gases. Cailteau et al[6] used FTIR and nondispersive infrared (NDIR) spectroscopy technique to measure the atmospheric trace species (CO_2, CH_4) under URL conditions. The quadrupole mass spectrometry (QMS) used by Tomonaga et al[4,5] to quantify the partial pressures of He, Ar, Kr, N_2, O_2, CO_2, and CH_4 in gaseous and aqueous matrices in Mont Terri URL (Switzerland) presents an analytical uncertainty of approximately 1% to 3%.

The aforementioned limitations of current technologies can be overcome using QMS and Picarro technology. Several QMS calibration methods for online gas composition measurement were proposed by many studies in various fields over the past decades.[4,5,11,15–26] Nevertheless, online analysis of complex mixtures consisting of several gases (noble gases, N_2, CO_2, CO, O_2, H_2S, hydrocarbons, etc.) at lower concentrations is still challenging. The parameters of the mass spectrometer that allow the quality and accuracy of the calibration to be assessed (sensitivity, linearity, stability, and repeatability) are difficult to control.[24,27] The QMS has low long-term stability;[22,23,28] therefore, its use requires a regular and accurate setup calibration phase. Another difficulty related to the use of the MS is the choice of characteristic peaks (m/z)[11,15,22,27] with as few interferences as possible. For a mixture composed of several gas species, the molecules are ionized and fragmented; these fragments are then separated based on their mass-to-charge ratio (m/z). Organic species fragment into several masses. Overlapping fragments at similar m/z values can make the identification of individual species difficult.[11,23,27]

The monitoring of the chemical evolution of the air in the URL's structures is performed in a matrix dominated by nitrogen.[4,5,8] A gas monitoring station "Flair Soil" has been designed to monitor the gaseous composition inside the Meuse/Haute-Marne URL, located at −490 m depth. This station brings together two analyzers: a QMS (HPR-20 R&D Hiden Analytical), which allows following the evolution of several gases, and an IR laser spectroscope (Picarro), which provides simultaneous measurements of CH_4, CO_2, and CO. For the optimal use of the mass spectrometer, a precise adjustment and calibration phase is necessary. The choice of a Hiden Analytical HPR-20 R&D QMS was motivated by the fact that this device allows the analysis of several gases in real time with a sampling time of a few seconds and the analysis is fast.

The biggest challenge overcome in this study is working with mixtures of several low-content gases with spectral interferences. These problems affect the accuracy and repeatability of MS measurements. The aim of this paper is to propose an analytical method to measure the gaseous composition of multiple molecules such as light hydrocarbons, noble gases, greenhouse gases, O_2, H_2, N_2, CO, and H_2S, unlike previous methods,[4,5,11,15,18,21] which are limited to a few molecules. This article presents a new method to calculate calibration coefficients and relative concentrations of gases in a nitrogen matrix despite multiple interferences and very low concentrations. This method belongs to the multivariate calibration class.[18,29,30] With regular corrections, this method has been optimized and validated for its ability to detect gases in complex mixtures at low concentrations with interferences, with acceptable errors. Finally, it can be used to monitor the chemical evolution of gases in different types of closed or partially closed underground structures in real time.

2 | MATERIALS AND METHODS

2.1 | Experimental scheme of Flair Soil

To monitor the composition of the gas contained in underground structures, a gas monitoring station called Flair Soil has been developed, which is composed of two analyzers: a QMS and a Picarro. The operating scheme of the Flair Soil used for MS calibration and online gas monitoring is shown in Figure 1B. The design of the gas circuit allows the connection of two gas cylinders. The first cylinder of the PCV40 Nitrogen line contains pure nitrogen; it is equipped with a manual pressure gauge allowing (a) to pilot the solenoid valves at 6 Bar (b) to purge the lines and to realize the background noises of the analyzers at approximately 1 Bar. The pressure of 6 Bar at the outlet of the regulator is reduced by 1 to 2 Bar by a two-way solenoid valve. The second line, PCV50 Standards, is dedicated to the measurement and circulation of standard gases. The standard gas cylinders are regulated in the range of 0.01–0.1 Bar depending on the desired total pressure in the mass spectrometer. The Flair Soil is composed of seven solenoid valves that allow the air (EV30 and EV31) or gas (EV41 and EV51) inlet to be opened and closed in the system. The EV10 and EV20 solenoid valves allow the air or gas supply to be opened and closed in the Picarro and the mass spectrometer, respectively. A pressure sensor, Keller Pressure Gauge (PI33), is used to measure and control the pressure evolution in the system. The two vacuum pumps, QMS (P-20) and Picarro (P-10), are connected at the outlet of the two analyzers and ensure the circulation of gas in the system and help maintain the vacuum. The calculated concentrations are displayed for both devices (HPR-20 Hiden and Picarro) on the right of the Flair Soil screen control in Figure 1B.

2.1.1 | IR laser spectroscopy, Picarro

The Picarro (G2401) is an analyzer equipped with an IR laser. It provides precise and simultaneous measurement of gases such as CH_4, CO_2, and CO at parts-per-million and water vapor. The principle

is based on CRDS, a technique that involves introducing a gas sample into a very fine optical cavity and determining the optical absorbance of the sample, which makes the measurement of the gas concentration possible.[13]

The gas concentration is measured at a pressure of ~187 mbar at 45°C (the measuring cavity). The Picarro has a gas supply flow rate of about 1.5 slm (standard liter per minute) at 1.013 Bar (atmospheric pressure). The Picarro was pumping too much air, and the initial flow rate was reduced from 1.5 slm by adding an orifice with a low flow rate at the outlet. The current flow rate of the measurement is approximately ~0.130 slm.

In this work, Picarro and mass spectrometer measurements are complementary. Picarro measures gases in very low concentrations. The measurement ranges of CO_2 are between 0% and 0.1%, CH_4 is between 0% and 0.002%, and CO is between 0% and 0.0005%.

2.1.2 | QMS, Hiden HPR-20 R&D

Mass spectrometry (MS) is an analytical technique that separates chemical species in a gas mixture based on their mass-to-charge ratio (m/z). It is used to detect and quantify atoms or molecules of an unknown gas sample.[31] The mass spectrometer implemented in this study is an HPR-20 R&D Hiden Analytical. It operates in dynamics under a secondary vacuum by means of turbomolecular pumping (lower than 10^{-5} mbar). The capillary with a diameter of 0.02 mm and a length of 2 m allows the gas to be sampled at atmospheric pressure and continuously at a flow rate of 0.002 slm. The capillary is heated to 200°C to evacuate water vapor. The molecules are introduced into the electron impact source (closed source) and are ionized by collision with the electrons emitted by a hot filament (oxide-coated iridium). The ionized species are then separated according to their mass-to-charge ratio by electrical scanning for quadrupole analyzers. The ions separated by the analyzer are then transformed into electric current (proportional to the number of ions) by means of two detectors, the Faraday cup and the electron multiplier (EM).

The choice of a Hiden Analytical HPR-20 R&D QMS was motivated by the fact that this device allows the analysis of several gases in real time with a sampling time of a few seconds and the analysis is fast. The Hiden HPR-20 R&D system is conceived for the detection of species from a concentration of less than 0.0005% to a concentration of 100% in a matter of seconds.[32] The analysis of the sample does not require any preparation or purification of the gas before introduction in the QMS.

The Hiden mass spectrometer is supplied with MASsoft software with which one can access all the features of the spectrometer and control external devices. In MASsoft software, several MS parameters can be adjusted depending on the acquisition method: selection of the detectors, voltage applied to the EM, focus plate, emission current, electron energy, and settle and dwell times. Using these parameters is a compromise between the sensitivity, the resolution, and the lifetime of the filaments.[32] After calibration, the values of these parameters remain unchanged. Any changes will result in adverse effects on sensitivity and repeatability[11,23] and will also require the calculation of new calibration coefficients.

2.2 | Quantitative detection method for MS

2.2.1 | Determination of interferences using databases MASsoft and NIST

Given the complexity of the mixtures analyzed in this study, one of the difficulties encountered was the choice of the best masses/peaks characteristic of each species. The ionization source used, electron impact, is very energetic and causes a significant fragmentation of molecular ions, resulting in the formation of complex fragmentation patterns especially for organic species. To overcome this problem, one can choose from the MASsoft or NIST databases, the noninterfering peaks, but it's challenging given the number of interferences that organic species may have. These difficulties were also reported in the literature.[11,27]

Table 1 shows the mass fragments used for the mass spectrometer analysis. For example, to avoid the interference of argon ($^{40}Ar^{++}$) with neon ($^{20}Ne^{+}$), the mass 20 of argon was removed by decreasing the ionization energy (48 eV) of neon. In general, for the calibration of pure gases, the most intense signal (base peak) can be selected, but for complex mixtures, the base peaks overlap with the peaks (spectral interferences) of other gases.[11,18,20,22] For the choice of masses, we preferred to refer to the library provided by the MASsoft software (for Hiden analyzers) because the values can differ based on the machines. Karlegärd et al[15] and Le et al[11] report that the more fragments used in the calibration matrix, the more complex the method, the more accurate the analysis, but the longer the measurement time. Therefore, in the present work, to reduce the complexity of the method and improve the speed and accuracy of the analysis method, fewer mass fragments are used. Table 1 presents the best mass-to-charge ratios chosen for each gas under the experimental conditions described in this study.

As is common in MS data analysis,[11,18,22,27] in this study, linearity tests were carried out with gases whose presence is expected in the URL. Standard mixtures, which constituted simple mixtures and complex mixtures, were analyzed to determine which peaks performed best in terms of response linearity and signal intensity. For both low and high concentrations, linearity between relative gas concentrations and ion currents was verified for all gases.

2.2.2 | Preparation of simple two-component and complex multicomponent gas mixtures

Two types of mixtures were used for the development of this method: (a) simple mixtures, that is, a pure gas in a nitrogen matrix; and (b) complex mixtures, that is, multiple gases in a nitrogen matrix. Pure nitrogen (100%) exerts background noise under the same

TABLE 1 Construction of the *m/z* matrix based on the molecules of interest and the spectral interferences (crosses = masses) on the measured mass-to-charge ratios (*m/z*)

m/z	H_2	He	N_2	CH_4	Ne	C_2H_4	C_2H_6	O_2	H_2S	C_3H_6	C_3H_8	Ar	CO_2	*i*-C_4H_{10}	*n*-C_4H_{10}	C_5H_{12}
2	X															
4		X														
14			X													
15				X							X			X	X	
20					X											
27						X	X			X	X			X		X
30							X				X			X		
32								X	X							
34								X	X							
38										X	X	X		X	X	X
39										X	X			X	X	X
40												X				
46													X			
57														X	X	X
58														X	X	
72																X

Note: The main ion currents (mass = *m/z*) chosen for each gas are in green and the interferences associated with each mass in orange.

conditions as when analyzing a sample and therefore has a zero of all chemical species. It serves as a "blank" and purges the system. Nitrogen constitutes our matrix. All gases used in this study were purchased from AirProducts (Leonardo Da Vincilaan, Diegem, Belgium) and supplied with the molar % (mol.%) compositions, with uncertainties between ±0.2% and ±5% on each of the relative concentration values (S1 to S10 and T1 and T2). The compositions of the gases used for the calibration of the mass spectrometer are presented in Table 2, and those used to assess the uncertainty/accuracy of the method are presented in Table 3. Standards S1 to S10 (10 gas bottles) are mixtures composed of interest gases in a nitrogen matrix. These mixtures have been chosen to have no (or less) mass interference to calculate calibration coefficients and determine the contribution of each individual interfering ionized species to the global signal. The two standards (two gas bottles), T1 and T2, are complex mixtures in a nitrogen matrix; they have isobaric interference and have been treated as unknown samples and used to assess the accuracy and the repeatability of the method.

2.2.3 | Experimental workflow for a gas quantification method

The measurement procedure is as follows:

1. A "blank" (background) measurement is carried out with pure nitrogen (100%), that is, with a pressure corresponding to the standard pressure during the experiment. This enables defining the background (noise), that is, the level of residual gas in the system for the gases of interest.
2. The *calibration* measurement is carried out from the whole standard mixture (S1 to S10), always at relatively constant pressure. The "blank" is passed between each mixture if the measurements are not performed successively.
3. The measurement of the *experiment* (T1 and T2, atmospheric air, gases in micro-tunnels and boreholes, etc.) (samples) is carried out, always at constant pressure.

The data postprocessing procedure is as follows:

1. The ion currents (partial pressures) are normalized by the total pressure of the mass spectrometer (vacuum operating pressure).
2. Next, the *background* measurement for each gas is averaged over the last points (10, 20, 30, or so), depending on the desired accuracy.
3. Then, the *calibration* and *experiment* for each gas are averaged over the last points (10, 20, 30, or so). The average value of the background is subtracted from the calibration and experiment values.
4. Finally, the calibration coefficients are determined, and then these coefficients are applied to the experimental values to determine the quantitative values of each gas.

2.2.4 | Calculation of calibration coefficients and building of the matrix based on the molecules of interest

The mathematical approaches,[11,20,23,25,27] in particular, matrix calculations,[18] provide qualitative and quantitative information from mass spectra. These methods assume that the measured ion currents

TABLE 2 Compositions of the different gas mixtures, S1 to S10, used in the calibration procedure

Standards	H_2 (mol.%)	He (mol.%)	CH_4 (mol.%)	Ne (mol.%)	N_2 (mol.%)	C_2H_4 (mol.%)	C_2H_6 (mol.%)	O_2 (mol.%)	H_2S (mol.%)	C_3H_6 (mol.%)	C_3H_8 (mol.%)	Ar (mol. %)	CO_2 (mol.%)	*i*-C_4H_{10} (mol.%)	*n*-C_4H_{10} (mol.%)	C_5H_{12}
Blank	0	0	0	0	100	0	0	0	0	0	0	0	0	0	0	0
S1	0.10	0.10	0.10	0	98.6	0	0	1.00	0	0	0	0	0.10	0	0	0
S2	0	0	0	0	99.9	0	0	0	0	0	0	0	0	0.05	0	0
S3	0	0	0	0	99.9	0	0	0	0.001	0	0	0	0	0	0	0
S4	0	0	0	0	99.5	0	0.50	0	0	0	0	0	0	0	0	0
S5	0	0	0	0	99.9	0.01	0	0	0	0	0	0	0	0	0	0
S6	0	0	0	0	99.9	0	0	0	0	0	0	0	0	0	0.01	0
S7	0	0	0	0	99.9	0	0	0	0	0	0	0	0	0	0	0.01
S8	0	0	0	0	99.9	0	0	0	0	0	0.05	0	0	0	0	0
S9	0	1.01	0	0.99	96.99	0	0	0	0	0	0	1.02	0	0	0	0
S10	0	0	0	0	99.9	0	0	0	0	0.01	0	0	0	0	0	0

TABLE 3 Compositions of the different test gas mixtures, T1 to T2, used for assessing the uncertainty and accuracy of the method

Tests	H_2 (mol.%)	He (mol.%)	CH_4 (mol.%)	Ne (mol.%)	N_2 (mol.%)	C_2H_4 (mol.%)	C_2H_6 (mol.%)	O_2 (mol.%)	H_2S (mol.%)	C_3H_6 (mol.%)	C_3H_8 (mol.%)	Ar (mol.%)	CO_2 (mol.%)	i-C_4H_{10} (mol.%)	n-C_4H_{10} (mol.%)	C_5H_{12} (mol.%)
T1	0.051	0.005	0.001	0.049	99.74	0.001	0.001	0	0	0.001	0.001	0.100	0.050	0.001	0	0.001
T2	0.102	0.051	0.099	0.051	99.1	0.050	0.097	0.050	0.002	0.051	0.050	0.096	0.049	0.050	0.049	0.050

are linear for each pure component.[11,18,27] In this study, matrix calculations are offered to match chemical species to measured ion currents. Each ion current intensity y_i measured by the quadrupole is the function of all the chemical species (nature and concentration x_i) that constitute the analyzed gas. This function can be expressed as follows (1):

$$y_i = \sum_j a_{ij} x_j, \tag{1}$$

where a_{ij} is referred to as the response coefficient of the chemical species j on the ion current y_i, and x_j its concentration. The latter relation (1) assumes two fundamental hypotheses:

1. The ion current intensity is a linear function of each species concentration.
2. The contributions of all gases are independent (no crossed contributions) and add up.

As seen previously, the first hypothesis has been verified for low and high concentrations using gases with different contents (in this study). Equation (1) is written for all the measured ion currents y_i. It gives a system of n linear equations (n being the number of ion currents measured). This system is more simply described using a matrix representation (Equations [2] and [3]):

$$\begin{pmatrix} y_1 \\ \vdots \\ y_n \end{pmatrix} = \begin{pmatrix} a_{11} & \dots & a_{ik} \\ \vdots & \ddots & \vdots \\ a_{nj} & \dots & a_{nk} \end{pmatrix} \cdot \begin{pmatrix} x_1 \\ \vdots \\ x_k \end{pmatrix}, \tag{2}$$

$$\mathbf{Y} = \mathbf{A} \cdot \mathbf{X}. \tag{3}$$

In this system, **Y** represents the vector of the measured ion currents y_i (size n), **X** represents the vector of the relative concentration of the chemical species considered x_i (size k), and **A** represents the matrix containing all the calibration coefficients a_{ij} of each chemical species j on each of the ion currents y_i at the ith m/z (size $n \times$ k). Matrix **A** is referred to in the following text as the calibration matrix. The objective of the calibration is the determination of all the a_{ij} coefficients ($n \times k$ coefficients).

The calibration of matrix **A** is performed using standard gases, for which the chemical composition is known. Ion currents of each gas species have been obtained by analyzing in a nitrogen matrix each pure gas with known concentration. Three types of standards are used to calculate the calibration coefficients: (a) pure gas (i.e., pure nitrogen), (b) simple mixtures (i.e., C_2H_6 in N_2) for molecules of known concentrations with little or no interference between each other, and (c) complex mixtures (i.e., H_2, He, CO_2, CH_4, and O_2 in N_2 ; no interference) at different contents. The use of pure gases enables simplification of Equations (1)–(4). For a pure gas (i.e., pure nitrogen), the calibration coefficient is calculated by dividing the normalized ion current of the pure gas by its concentration (Equation [4]). For the last two mixtures, the calibration coefficient is calculated by dividing the normalized ion currents (i.e., this normalized ion current is subtracted from nitrogen-normalized ion current) by the known gas concentration. All the calibration coefficients were used to build the calibration matrix. This is easily explained by Equations (5)–(7):

$$y_i = a_{ij} \cdot x_j \rightarrow a_{ij} = \frac{y_i}{x_j}, \tag{4}$$

$$\frac{y_i}{\mathrm{TPS}} - \frac{y_{(i,\mathrm{N2})}}{\mathrm{TPS}} = a_{ij} \cdot x_j, \tag{5}$$

$$a_{ij} = \frac{\left(\frac{y_i}{\mathrm{TPS}} - \frac{y_{(i,\mathrm{N2})}}{\mathrm{TPS}}\right)}{x_j}. \tag{6}$$

An example of the calculation of the calibration coefficient (a_{ij}) for H_2 of $m/z = 2$ is given by Equation (7).

$$a_{H2,2} = \frac{\left(\frac{y_2}{\mathrm{TPS}} - \frac{y_{(2,\ \mathrm{N2})}}{\mathrm{TPS}}\right)}{x_{\mathrm{H2}}}. \tag{7}$$

In these equations, y_i represent the measured ion currents of the chemical species j and $y_{(i,\ \mathrm{N2})}$ those of nitrogen (N_2) at the ith m/z, a_{ij} is the calibration coefficient of the gaseous species considered, TPS represents the total pressure of the mass spectrometer, x_j is the known relative concentration, y_i/TPS is the *calibration* and *experiment* measurement, and $y_{(i,\ \mathrm{N2})}$/TPS is the *background* measurement normalized. The total pressure (TPS) may vary slightly depending on the standards analyzed.

2.2.5 | Checking the matrix with test gases T1 and T2

After calculating the calibration coefficients of each gas individually and separately in the nitrogen matrix, the calculated values are then input into the matrix system, which are used to calculate the relative concentrations from the measured ion currents of an assumed unknown standard(s), test gas T1 and T2, in the present work. The system of linear equations described previously must be inverted. With this method, we need to monitor as many ion currents as chemical species we are interested in (providing that these ion currents are correctly selected to avoid collinearity). With this condition ($n = k$), the matrix **A** is square and can be inverted (A^{-1}). The relative concentrations (X) can there be computed using Equation (8), while measuring the ion currents (Y) of the unknown gas mixture.

$$X = A^{-1} \cdot Y. \tag{8}$$

3 | RESULTS AND DISCUSSION

3.1 | Calibration matrix A

Results in Table 4 show that most of the coefficients are null, traducing the fact that a chemical species does not respond on all the ion current. For our system, which is composed of 16 equations and 16 chemical species, only 39 coefficients need to be determined (among the 16×16 coefficients). Similar systems have been described in the literature[11,15,18] with, however, less complex mixtures composed of fewer gases (gas types) and at higher concentrations than those used in this work (except for N_2). For example, Binninger et al[18] determined the gas concentration using the number of gas in the mixture ($k = 5$). Similar to their method, we optimized the number of gases in the mixture as $k = 16$.

Several chemical species can respond mainly on the same ion current. For example, the ion currents detected at $m/z = 30$ depend on the following gases: C_2H_6, C_3H_8, and i-C_4H_{10} due to their primary or secondary ionization products. The matrix **A** is globally upper triangular; that is, the terms of **A** below the diagonal are zero (when chemical species and ion currents are arranged by increasing atomic masses and m/z values, respectively). In Table 4, all light hydrocarbons show spectral interference with other hydrocarbons. H_2, He, Ne, and CO_2 are not affected by interference. Interference of N_2 with other gases has been minimized because it is the matrix and represents more than 99% of all standards except S4 (more than 96%).

3.2 | Drift correction of the measured ion currents

In this section, experimental artifacts or drifts that exist and may alter the result are discussed. Corrections of these effects are necessary to have a robust quantitative method. To consider the drift related to the pressure as much as possible, a relatively constant pressure must be maintained in the system. Decreases and increases in pressure, if they do not pose problems for the system, tend to vary the background noises, especially the one due to water vapor. The pressure is measured in the vacuum detector of the MS to be systematically normalized afterward. To compensate the drift, all ion currents are normalized with the total pressure in the MS during each corresponding measurement. This makes it possible to correct for drifts in calibration coefficients between different measurements, provided that these drifts are linearly related to the total pressure in the MS. This method is based on the assumption that the calibration matrix **A** is identical for all calibration measurements and independent of the gases present in the mixture.[18] Signal drift is a multivariate MS calibration methods problem and leads to deviations from the original calibration model.[23] In attempts to compensate the drifts, different normalization methods are frequently employed in the literature.[11,18,23,24,26] Such methods include the normalization to the sum of peaks, base peak, or an internal standard.

According to Turner et al,[23] for multivariate methods, normalization to the total ion current estimated by summing the peaks and normalization of the spectrum so the base peak equals to unity are not proved successful and are of questionable. Normalizing to a base peak would be incorrect, as the other peaks do not change in the same way. However, Le et al[11] successfully built their calibration method using normalization to the total ion current (internal standard). This method is based on comparing the signal intensity of the product to be quantified with that of a reference compound. To compensate for changes of the ion currents, Binninger et al[18] used the internal MS pressure for normalization to build their multivariate calibration methods. Pressure normalization has the advantage of being independent from the gases in the mixture. In the present work, normalizing to the total pressure of the MS was selected to build the multivariate calibration method.

Once the MS is well calibrated with the calculated reference values of the ion currents (Y_{ref}) of the test gases T1 or T2, it is necessary to analyze daily the same standard to determine $Y(t)$ (daily measurement). This analysis is performed to reduce the drifts on the measurements of ion currents. These slight drifts can be not only due to slight changes in the overall pressure of the system and degradation in the detector and ionization efficiency as reported in the literature[18,23] but also due to the ambient environment and the presence of water vapor. Y_{ref} is obtained by multiplying the matrix calibration coefficients by the test gases concentrations. When measuring $Y(t)$, it is important to ensure that there is not a large difference (less than one order of magnitude between the measurements) between Y_{ref} and $Y(t)$; otherwise new measurements of the test gas must be made. The graphical representation of $Y(t)$ as a function of Y_{ref} enables the deduction of the correction factor, a, from a regression line (Figures 2A and 2B). To correct the drift observed in all measured ion currents, different possibilities were considered: (a) a correction in the form of $Y_{corr}(t) = Y(t)/a$ and (b) $Y_{corr}(t) = Y(t) * a$. After several tests, it appeared that $Y_{corr}(t) = Y(t)/a$ gave good results, so the latter was used to build the method. During the correction process, not all the gases were corrected in the same way. H_2, N_2, CH_4, and C_2H_4 were corrected by considering the N_2 in the mixture when plotting the correction line (Figure 2A). For the other gases, N_2 was not considered when plotting the correction line (Figure 2B). After several tests, the test gas T2 was chosen because it contains all the gases used in this study with similar concentrations to those expected in the planned experiments. As commonly done in MS data analysis,[15,18,20,21] for best accuracy and feasibility, it is advisable to use calibration concentrations that are close to the experimental concentrations of a mixture considered as unknown. This calibration approach can be applied to any other measurement and in various environments. Equation (9) is used to correct the drift observed on the ion currents measured daily. $Y_{corr}(t)$ is the corrected ion current.

$$Y_{corr}(t) = \frac{Y(t)}{a}. \quad (9)$$

After correcting the drifts on the ion currents from Equation (9), the relative concentrations can then be calculated using Equation (10).

TABLE 4 Representation of matrix **A** with all interferences

IC	H_2	He	N_2	CH_4	Ne	C_2H_4	C_2H_6	O_2	H_2S	C_3H_6	C_3H_8	Ar	CO_2	i-C_4H_{10}	n-C_4H_{10}	C_5H_{12}
y_2	#####	0	0	0	0	0	0	0	0	0	0	0	0	0	0	0
y_4	0	1.87E−03	0	0	0	0	0	0	0	0	0	0	0	0	0	0
y_{14}	0	0	4.55E−04	0	0	0	0	0	0	0	0	0	0	0	0	0
y_{15}	0	0	0	1.22E−02	0	0	0	0	0	0	2.32E−03	0	0	2.19E−03	6.30E−03	0
y_{20}	0	0	0	0	4.02E−03	0	0	0	0	0	0	0	0	0	0	0
y_{27}	0	0	0	0	0	1.10E−02	7.18E−03	0	0	6.58E−03	7.49E−03	0	0	6.56E−03	0	7.16E−03
y_{30}	0	0	0	0	0	0	5.89E−03	0	0	0	8.56E−04	0	0	2.68E−04	0	0
y_{32}	0	0	0	0	0	0	0	5.42E−03	3.92E−02	0	0	0	0	0	0	0
y_{34}	0	0	0	0	0	0	0	7.26E−05	8.27E−03	0	0	0	0	0	0	0
y_{38}	0	0	0	0	0	0	0	0	0	2.63E−03	9.19E−04	1.52E−05	0	6.01E−04	4.37E−04	3.89E−04
y_{39}	0	0	0	0	0	0	0	0	0	1.16E−02	3.23E−03	0	0	3.90E−03	3.38E−03	3.99E−03
y_{40}	0	0	0	0	0	0	0	0	0	0	0	2.60E−02	0	0	0	0
y_{46}	0	0	0	0	0	0	0	0	0	0	0	0	1.04E−04	0	0	0
y_{57}	0	0	0	0	0	0	0	0	0	0	0	0	0	9.15E−04	8.21E−04	8.72E−03
y_{58}	0	0	0	0	0	0	0	0	0	0	0	0	0	9.01E−04	3.69E−03	0
y_{72}	0	0	0	0	0	0	0	0	0	0	0	0	0	0	0	1.31E−03

Note: Ion currents (y_i) measured at the ith m/z that exhibit spectral interference are y_{15} (i.e., CH_4, C_3H_8, i-C_4H_{10}, and n-C_4H_{10}), y_{30} (i.e., C_2H_6, C_3H_8, and i-C_4H_{10}), y_{39} (i.e., C_3H_6, C_3H_8, i-C_4H_{10}, n-C_4H_{10}, and C_5H_{12}), y_{57} (i.e., i-C_4H_{10}, n-C_4H_{10}, and C_5H_{12}), and y_{58} (i.e., i-C_4H_{10} and n-C_4H_{10}). Bold is for legibility. Green represents the main masses, and orange represents the associated interferences.

Abbreviation: IC, ion current.

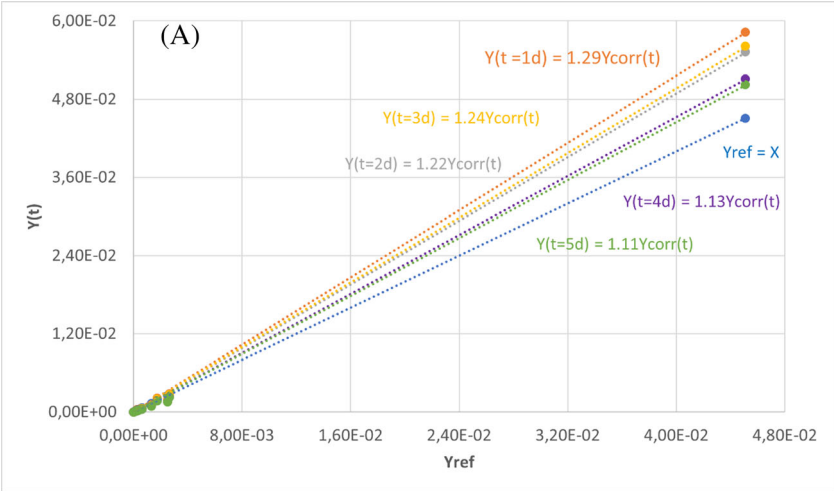

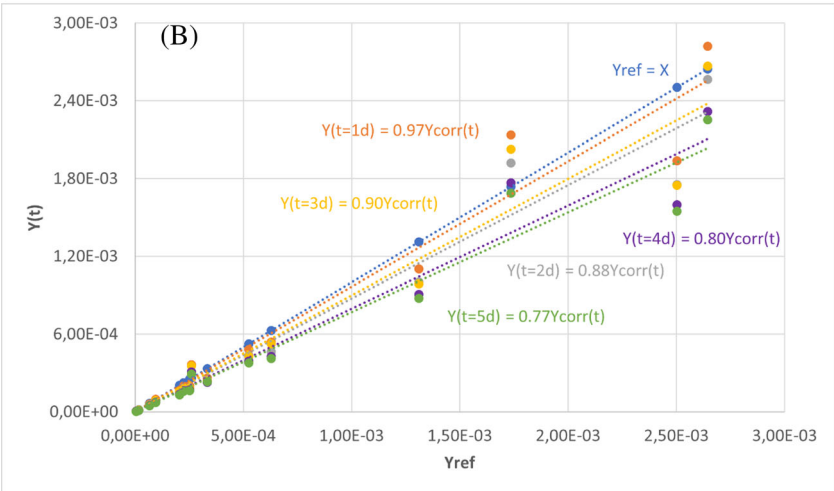

FIGURE 2 Representation of $Y(t)$ as a function of Y_{ref} for the determination of the correction factor a (the measurements were performed for 5 days). A, Correction taking into account the nitrogen in the plotting of the correction line. B, Correction without considering the nitrogen in the plotting of the correction line [Color figure can be viewed at wileyonlinelibrary.com]

$$X(t) = A^{-1}.Y_{corr}(t). \quad (10)$$

3.3 | Assessment of quantitative detection quality of interfering and noninterfering gases

First, the MS was calibrated with multivariate calibration method using the calibration mixtures S1 to S10. Second, test gas mixtures T1 and T2 with known concentrations were measured with the calibrated MS system to assess the quality of the calibration. After calculating all the calibration coefficients for each chemical species (Sections 2.2.4 and 2.2.5), these values are introduced into the calculation matrix (**A**). The calibration matrix **A** is then reversed, and the relative concentrations of an unknown mixture are calculated by multiplying the corrected ion currents $Y_{corr}(t)$ of the unknown mixture with the inverse of the calibration matrix **A**. The concentrations obtained by this method and those determined by the supplier (AirProducts) are shown in Tables 5 and 6 for test gases T1 and T2, respectively. The values represented in Table 5 (3-day averages) and Table 6 (3-month averages) are average values of relative concentrations obtained after the correction. The results are in good agreement with those of the supplier (with supplier uncertainties ranging between ±0.2% and ±5%

TABLE 5 Results of measurement and respective SDs for test gas mixture T1 obtained in the Meuse/Haute-Marne Underground Research Laboratory

Gases	Supplier (mol.%)	Calculated concentrations (mol.%)
H_2	0.051 (±1)	0.042 (±0.006)
He	0.005 (±2)	0.007 (±0.000)
N_2	99.74 (±0.2)	99.86 (±0.01)
CH_4	0.001 (±2)	0.002 (±0.001)
Ne	0.049 (±1)	0.051 (±0.003)
C_2H_4	0.001 (±2)	0
C_2H_6	0.001 (±2)	0.003 (±0.001)
O_2	0	0
H_2S	0	0
C_3H_6	0.001 (±2)	0.001 (±0.000)
C_3H_8	0.001 (±2)	0.001 (±0.001)
Ar	0.100 (±5)	0.100 (±0.000)
CO_2	0.050 (±1)	0.063 (±0.001)
i-C_4H_{10}	0.001 (±2)	0.001 (±0.000)
n-C_4H_{10}	0	0
C_5H_{12}	0.001 (±1)	0.001 (±0.000)

Note: These values represent 3-day averages of relative concentrations obtained after the correction. The uncertainties associated with the supplier's values are also presented.

TABLE 6 Results of measurement and respective SDs for test gas mixture T2 obtained in the Meuse/Haute-Marne Underground Research Laboratory

Gases	Supplier (mol.%)	Calculated concentrations (mol.%)
H_2	0.102 (±3)	0.111 (±0.009)
He	0.051 (±1)	0.050 (±0.002)
N_2	99.10 (±0.2)	99.36 (±0.05)
CH_4	0.099 (±0.5)	0.090 (±0.012)
Ne	0.051 (±1)	0.042 (±0.001)
C_2H_4	0.050 (±0.5)	0.061 (±0.012)
C_2H_6	0.097 (±0.5)	0.086 (±0.005)
O_2	0.050 (±1)	0.040 (±0.005)
H_2S	0.002 (±5)	0.001 (±0.000)
C_3H_6	0.051 (±0.5)	0.036 (±0.010)
C_3H_8	0.050 (±0.5)	0.043 (±0.019)
Ar	0.096 (±2)	0.080 (±0.005)
CO_2	0.049 (±0.5)	0.047 (±0.002)
i-C_4H_{10}	0.050 (±0.5)	0.073 (±0.019)
n-C_4H_{10}	0.049 (±0.5)	0.039 (±0.006)
C_5H_{12}	0.050 (±0.5)	0.047 (±0.004)

Note: These values represent 3-month averages of relative concentrations obtained after the correction. The uncertainties associated with the supplier's values are also presented.

on each of the relative concentration values). The sum of the concentrations obtained is slightly greater than 100% (100.13% for T1 and 100.20% for T2); this is because some of the gases are slightly overdetermined, the slight changes of the overall pressure of the system can also lead to small deviations of the total sum of the relative concentrations. Similar changes were observed in the literature.[11,18,23] For the sum to be equal to 100%, the relative concentrations obtained are normalized using a common factor.[18] The two test gas mixtures, T1 and T2, show that the SDs obtained by several repetitions of the overall calibration and test procedure are close to zero, meaning that the data are less dispersed from the mean. The very small SDs observed despite a time interval of 3 months on the measurements reveal a very good reproducibility of the obtained results. From the analysis of these results, it appears that the lower the concentrations, the larger the relative error of the measurements. This is even more true for light hydrocarbons, and the results are in agreement with the conclusions of Mbaegbu et al.[21]

Figure 3A shows the test gas T1 results obtained on September 8, 13, and 19, 2022, after making the corrections. The fact that the concentrations are less well determined is because the concentrations are lower and fall within the limits of quantification (LOQ) of this method (Table 7). Figure 3B shows the test gas T2 results obtained on September, November, and December 2022 after correction with the reference ion currents. The errors are more important for interfering gases (e.g., O_2, C_3H_6, C_3H_8, i-C_4H_{10}, and n-C_4H_{10}) in the mixture. The results are globally in agreement with those of the supplier. He, H_2S, CO_2, and C_5H_{12} are best determined in the test gas T2.

The major challenge faced in this study is working with mixtures of several low-content gases with interferences. In gas mixtures, interferences and low concentrations of the component generate problems. These problems affect the accuracy and repeatability of MS measurement. The multivariate calibration method developed in this work addresses and solves these problems by identifying the best peaks that should be used to detect all gases in the mixture. Our results suggest that using the mass fragments of m/z in Table 1 can help detect light hydrocarbons, noble gases, sulfides, greenhouse gases, oxygen, hydrogen, and nitrogen in the same mixture (Figures 3A and 3B). However, the masses selected may be identical or different depending on the methods and experimental conditions. For example, Mbaegbu et al[21] selected the following masses: 15, 26, 41, 43, and 73 for CH_4, C_2H_6, C_3H_8, C_4H_{10}, and C_5H_{12}, respectively, to detect hydrocarbons from gas streams in live well fluids. Li et al[17] used the m/z fragments of 2, 32, 40, and 44 for H_2, O_2, Ar, and CO_2 in their method. To develop their method, Binninger et al[18] selected masses 2, 14, 28, 40, and 44 for H_2, N_2, CO, and CO_2 in Ar, taking into account interference between different gases. Considering interferences, Le et al[11] selected mass fragments of m/z 2, 15, 14, 28, 32, 34, and 44 for H_2, CH_4, N_2, CO, O_2, H_2S, and CO_2, respectively. From gasification gas, Karlegärd et al[15] selected mass fragments of m/z 2, 15, 14, 28, 32, 34, 40, and 44 for H_2, CH_4, CO, N_2, O_2, H_2S, Ar, and CO_2. During online monitoring of the gas composition (H_2, He, CH_4, N_2, O_2, Ar, and CO_2) in Mont Terri URL, Tomonaga et al[4,5] used peaks 2, 4, 15, 28, 32, 40, and 44, respectively. Some of the mass fragments used by the different authors mentioned earlier are identical to those used in this study, whereas others are different.

3.4 | Checking repeatability

The repeatability was checked over a 3-month period, and the values are presented in Figure 4 and Table 6. Figure 4 shows the evolution of the calculated test gas T2 concentrations from September to December 2022. Each chemical species is represented by a different color (see caption). The analysis of this graph shows a slight drift in general for all gas concentrations, except for hydrogen sulfide. As mentioned in Section 3.2, these drifts can be due to multiple factors. As shown by the very small SD values (less than 0.06 mol.%) in Table 6, the results obtained by this method are reproducible and repeatable. This is confirmed by Figure 4, which shows the evolution of the results over 3 months without the observation of a significant variation. The SDs of 0.08 mol.% are reported by Binninger et al.[18]

3.5 | Determination of the limit of detection and limit of quantification of the method in term of ion currents and relative concentrations

The smallest signal (mass or concentration) of substance, here gas, detectable (which can be reliably distinguished from blank) but not quantifiable with acceptable uncertainty corresponds to the limit of

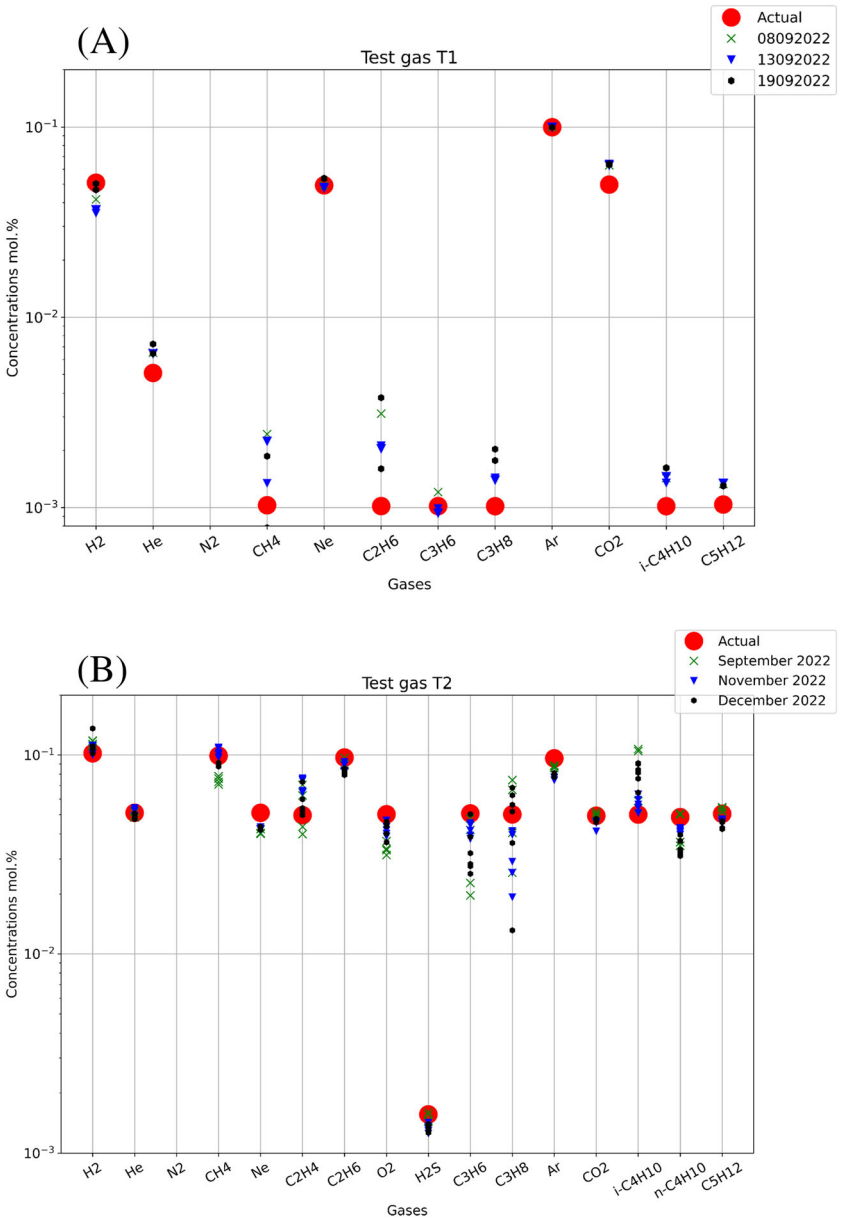

FIGURE 3 Actual concentrations given by the supplier and the values obtained by this method. A, Illustration of the results obtained on September 8, 13, and 19, 2022; and B, results over a 3-month period: September, November, and December 2022, after correction with the reference ion currents. The size of the symbols (dot, cross, inverted triangle, and hexagon) does not take into account the uncertainty of the measurement. The red dots represent the actual concentrations given by the supplier; the green cross, the inverted blue triangle, and the black hexagon represent the values obtained after correction. For a better readability, nitrogen, which represents more than 99% of the content, is not represented on this figure [Color figure can be viewed at wileyonlinelibrary.com]

detection (LOD). The LOQ corresponds to the smallest signal, mass, or concentration (value quantified with good precision) with an acceptable degree of certainty.[33,34] Both terms do not take into account interferences. The LOD and LOQ of this calibration method were determined directly by repeated measurement of the blank (i.e., nitrogen), knowing the mean and SD, according to Equations (11) and (12):

$$LOD = m_{\text{blank}} + k\, s_{\text{blank}}, \tag{11}$$

$$LOQ = m_{\text{blank}} + 10\, s_{\text{blank}}, \tag{12}$$

where m_{blank} and s_{blank} are the mean and SD of the measurements of the blank, respectively, and k is a numerical factor chosen according to the desired confidence level. In general, k equals 3.

As commonly done in the International Union of Pure and Applied Chemistry (IUPAC), we have used a value of 3 for the factor k. This factor corresponds to a probability of 0.13%, concluding that the sample analyzed contains the substance of interest while it is absent. The value of 10 for LOQ represents the measurements of 10 independent blanks and corresponds to a probability of 0.05%. This concludes that the sample contains a desired substance when this substance is not present.

First, the LOD and LOQ were calculated using the ion currents of the 10-nitrogen blank, and then the concentrations were calculated. Thus, the concentration is obtained by dividing (the ion currents of the 10 blanks) the LOD (13) or the LOQ (14) by the calibration factors obtained from the measurement of each gas individually in a nitrogen matrix. However, one must be cautious: indeed, these results depend on many conditions such as slight fluctuations in the total pressure of the MS and the measurement of ion currents at a given mass m/z

TABLE 7 Results of the calculation of the limit of detection (LOD) and limit of quantification (LOQ) in terms of ion currents and relative concentrations

Ion currents	LOD_y	LOQ_y	T1	T2	C_j (ppm) LOD_y	C_j (ppm) LOQ_y
y_2	7.87E−11	2.01E−10	3.65E−10	5.37E−10	177.89	453.57
y_4	6.66E−14	6.58E−14	1.70E−11	1.22E−10	0.20	0.22
y_{15}	6.62E−10	9.57E−10	6.39E−10	3.40E−09	313.59	445.95
y_{20}	2.19E−11	4.50E−11	3.13E−10	2.28E−10	31.50	64.55
y_{27}	7.28E−11	1.06E−10	1.32E−10	3.94E−09	38.22	55.25
y_{30}	2.45E−10	3.46E−10	2.20E−10	8.76E−10	240.38	336.47
y_{32}	1.10E−10	2.46E−10	4.39E−11	4.55E−10	117.31	260.89
y_{34}	5.14E−12	1.44E−11	7.18E−13	1.89E−11	3.62	10.15
y_{38}	1.05E−12	2.07E−12	1.00E−11	2.83E−10	2.32	4.55
y_{39}	2.47E−12	6.13E−12	3.79E−11	1.51E−09	4.50	11.23
y_{40}	5.92E−10	1.07E−09	4.15E−09	2.92E−09	133.04	241.19
y_{46}	1.93E−12	4.16E−12	9.79E−12	6.78E−12	107.75	231.85
y_{57}	1.26E−12	3.52E−12	1.84E−11	6.54E−10	8.09	22.60
y_{58}	2.80E−12	8.21E−12	2.67E−12	2.71E−10	4.42	12.98
y_{72}	2.52E−13	6.83E−13	2.45E−12	8.05E−11	1.13	3.07

Note: The ion currents of the test gases T1 and T2 are also presented.

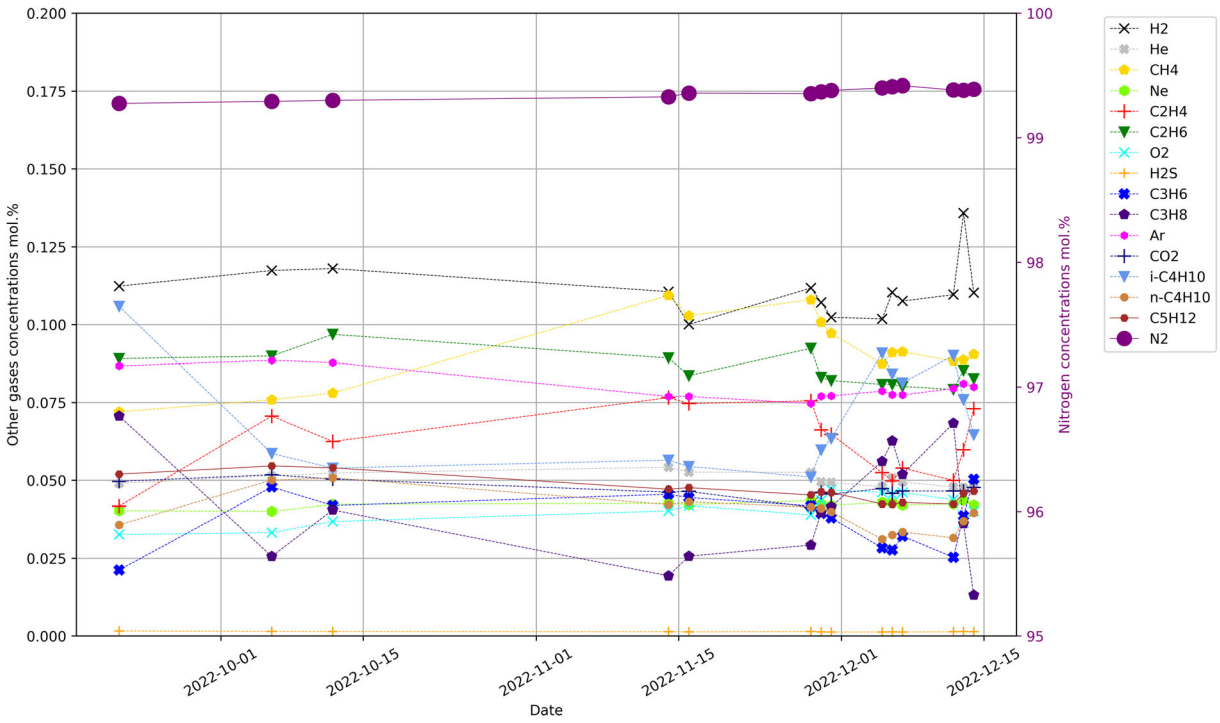

FIGURE 4 Evolution of test gas T2 concentrations calculated from September to December 2022 with slight variation [Color figure can be viewed at wileyonlinelibrary.com]

without spectral interferences, which can influence the calculation of the calibration coefficients and thus the calculation of relative concentrations.

$$C_j = \frac{LOD_y}{a_{ij}}, \tag{13}$$

$$C_j = \frac{LOQ_y}{a_{ij}}, \tag{14}$$

where C_j is the concentration of species j, LOD_y and LOQ_y are the LOD and the LOQ obtained from the measurement of the 10 ion currents of the 10 blanks, and a_{ij} is the calibration coefficient (Table 4).

Table 9 shows the ion current values and relative concentrations below which the gases may not be accurately detected and quantified. Determining the LOD and LOQ was also a challenge. For some gases, the concentration is low, and the signals (ionic currents) detected are below the LOQ_y and the LOQ_y of the background. Given the low gas concentrations involved, this was an important factor in the development of this method. The main objective was to validate the MS method's ability to accurately detect and quantify gases at lower concentrations (≈0.001%). As done by Mbaegbu et al,[21] the relative standard deviation (%RSD) with respect to concentrations was determined as the main validation criteria of the method. Hydrocarbons and other low-concentration gases were found to have the highest %RSD values. The values were greater than %RSD values of higher concentrations because, at a higher concentration, gas analysis by MS becomes easier. Calculation of %RSD and uncertainties for different gases at different concentration ranges has shown that lower concentrations of light hydrocarbons can lead to greater uncertainty in measurements. This is in line with the previous studies.[21] Our results show that the multivariate MS calibration method allows us to distinguish interfering and noninterfering gases with high accuracy, which is competitive with other gas analysis techniques.

4 | CONCLUSION

Using QMS coupled to Picarro G2401 gas concentration analyzer, an online and real-time quantitative detection method was developed and successfully tested to measure light hydrocarbons, noble gases, H_2S, greenhouse gases, O_2, H_2, and N_2 in closed microtunnels.

AUTHOR CONTRIBUTIONS

Seny Keita: Conceptualization; data curation; formal analysis; investigation; methodology; project administration; software; supervision; validation; visualization; writing—original draft; writing—review and editing. **Sonia Noirez:** Conceptualization; formal analysis; investigation; methodology; project administration; supervision; validation; visualization; writing—original draft. **Guillaume Berthe:** Conceptualization; funding acquisition; investigation; methodology; project administration; resources; supervision; validation; visualization; writing—original draft. **Agnes Vinsot:** Conceptualization; funding acquisition; investigation; project administration; resources; supervision; validation; visualization; writing—original draft; writing—review and editing. **Byeong Seok Kim:** Conceptualization; formal analysis; investigation; methodology; software; supervision; validation; visualization; writing—original draft. **Matthieu Mascle:** Conceptualization; data curation; formal analysis; methodology; software; supervision; validation; visualization; writing—original draft. **Mélanie Lundy:** Investigation; project administration; supervision; validation; visualization; writing—original draft; writing—review and editing. **Bruno Garcia:** Conceptualization; funding acquisition; investigation; project administration; resources; supervision; validation; visualization; writing—original draft.

ACKNOWLEDGMENTS

This work was financially supported by IFP Energies Nouvelles and the Agence Nationale pour la Gestion des Déchets Radioactifs.

PEER REVIEW

The peer review history for this article is available at https://www.webofscience.com/api/gateway/wos/peer-review/10.1002/rcm.9614.

DATA AVAILABILITY STATEMENT

Data available on request from the authors.

ORCID

Seny Keita https://orcid.org/0009-0007-2943-539X
Agnes Vinsot https://orcid.org/0000-0002-8332-5534

REFERENCES

1. Vinsot A, Lundy M, Linard Y. O_2 consumption and CO_2 production at Callovian-Oxfordian rock surfaces. *Procedia Earth Planet Sci*. 2017;17:562-565. doi:10.1016/j.proeps.2016.12.142
2. Libert M, Bildstein O, Esnault L, Jullien M, Sellier R. Molecular hydrogen: an abundant energy source for bacterial activity in nuclear waste repositories. *Phys Chem Earth, Parts A/B/C*. 2011;36(17–18):1616-1623. doi:10.1016/j.pce.2011.10.010
3. Vinsot A, Leveau F, Bouchet A, Arnould A. Oxidation front and oxygen transfer in the fractured zone surrounding the Meuse/Haute-Marne URL drifts in the Callovian–Oxfordian argillaceous rock. *Geol Soc, London, Spec Publ*. 2014;400(1):207-220. doi:10.1144/SP400.37
4. Tomonaga Y, Giroud N, Brennwald MS, et al. On-line monitoring of the gas composition in the Full-scale Emplacement experiment at Mont Terri (Switzerland). *Appl Geochem*. 2019;100:234-243. doi:10.1016/j.apgeochem.2018.11.015
5. Tomonaga Y, Wersin P, Rufer D, et al. Gas-bentonite interactions: towards a better understanding of gas dynamics in Engineered Barrier Systems. *Appl Geochem*. 2022;138:105205. doi:10.1016/j.apgeochem.2022.105205
6. Cailteau C, Pironon J, de Donato P, et al. FT-IR metrology aspects for on-line monitoring of CO_2 and CH_4 in underground laboratory conditions. *Anal Methods*. 2011;3(4):877-887. doi:10.1039/c0ay00623h
7. Vinsot A, Appelo C, Cailteau C, et al. CO_2 data on gas and pore water sampled in situ in the Opalinus Clay at the Mont Terri rock laboratory. *Phys Chem Earth, Parts A/B/C*. 2008;33:S54-S60. doi:10.1016/j.pce.2008.10.050
8. Vinsot A, Appelo CAJ, Lundy M, et al. Natural gas extraction and artificial gas injection experiments in Opalinus Clay, Mont Terri rock laboratory (Switzerland). *Swiss J Geosci*. 2017;110(1):375-390. doi:10.1007/s00015-016-0244-1
9. Vinsot A, Appelo CAJ, Lundy M, et al. In situ diffusion test of hydrogen gas in the Opalinus Clay. *Geol Soc, London, Special Publications*. 2014;400(1):563-578. doi:10.1144/SP400.12
10. Wicker T. Maximize mass spectrometer mud gas data—experienced analysis matters; #41623. 2015.
11. Le CD, Kolaczkowski ST, McClymont D. Using quadrupole mass spectrometry for on-line gas analysis—gasification of biomass and refuse derived fuel. *Fuel*. 2015;139:337-345. doi:10.1016/j.fuel.2014.09.010
12. Drake GWF. *Springer Handbook of Atomic, Molecular, and Optical Physics*. Springer; 2006. doi:10.1007/978-0-387-26308-3
13. Crosson ER. A cavity ring-down analyzer for measuring atmospheric levels of methane, carbon dioxide, and water vapor. *Appl Phys B*. 2008;92(3):403-408. doi:10.1007/s00340-008-3135-y

14. Konopel'ko LA, Beloborodov VV, Rumyantsev DV, Chubchenko YK, Elizarov VV. Metrological problems of gas analyzers based on wavelength-scanned cavity ring-down spectroscopy. *Opt Spectrosc*. 2015;118(6):1017-1022. doi:10.1134/S0030400X15060120
15. Karlegärd Å, Götz A, Bjerle I. On-line mass spectrometer analysis of gasification gas. *Chem Eng Technol Ind Chem Plant Equipment Proc Eng Biotechnol*. 1995;18(3):183-192. doi:10.1002/ceat.270180307
16. Robert E. Mass spectrometer calibration over wide concentration ranges in multicomponent gas mixtures. *Meas Sci Technol*. 2010;21(2):25102. doi:10.1088/0957-0233/21/2/025102
17. Li Q, Wang T, Wang D. Calibration of a mass spectrometer for the direct measurement of water concentration and its application to the study of sooting flames. *Meas Sci Technol*. 2012;23(5):55001. doi:10.1088/0957-0233/23/5/055001
18. Binninger T, Pribyl B, Pătru A, Ruettimann P, Bjelić S, Schmidt TJ. Multivariate calibration method for mass spectrometry of interfering gases such as mixtures of CO, N_2, and CO_2. *J Mass Spectrom*. 2018;53(12):1214-1221. doi:10.1002/jms.4299
19. Ellefson RE. Methods for in situ QMS calibration for partial pressure and composition analysis. *Vacuum*. 2014;101:423-432. doi:10.1016/j.vacuum.2013.08.011
20. Cheng Z, Mozammel T, Patel J, et al. A method for the quantitative analysis of gaseous mixtures by online mass spectrometry. *Int J Mass Spectrom*. 2018;434:23-28. doi:10.1016/j.ijms.2018.09.002
21. Mbaegbu MF, Adhikari PL, Gupta I, Rowe M. Mass spectrometric calibration procedure for real-time detection of lighter hydrocarbons. *Energies*. 2021;14(8):2123. doi:10.3390/en14082123
22. Sun W, Wu C, Cheng Y, et al. Study on calibrating the quadrupole mass spectrometers with gas mixture. *Measurement*. 2020;164:108099. doi:10.1016/j.measurement.2020.108099
23. Turner P, Taylor S, Clarke E, Harwood C, Cooke K, Frampton H. Calibration effects during natural gas analysis using a quadrupole mass spectrometer. *TrAC Trends Anal Chem*. 2004;23(4):281-287. doi:10.1016/S0165-9936(04)00403-0
24. Cook KD, Bennett KH, Haddix ML. On-line mass spectrometry: a faster route to process monitoring and control. *Ind Eng Chem Res*. 1999;38(4):1192-1204. doi:10.1021/ie9707984
25. Kaiser RI, Jansen P, Petersen K, Roessler K. On line and in sifu quantification of gas mixtures by matrix interval algebra assisted quadrupole mass spectrometry. *Rev Sci Instrum*. 1995;66(11):5226-5231. doi:10.1063/1.1146089
26. Bennett KH, Cook KD, Seebach GL. Simultaneous analysis of butene isomer mixtures using process mass spectrometry. *J Am Chem Soc*. 2000;11(12):1079-1085. doi:10.1016/S1044-0305(00)00182-3
27. de Hoffmann E, Stroobant V. *Mass Spectrometry: Principles and Applications*. 3rded. J. Wiley; 2007.
28. Yoshida H, Arai K, Akimichi H, Hirata M. Stability tests of quadrupole mass spectrometer by two-stage flow-dividing system. *Vacuum*. 2010;85(1):78-83. doi:10.1016/j.vacuum.2010.04.005
29. Beebe KR, Kowalski BR. An introduction to multivariate calibration and analysis. *Anal Chem*. 1987;59(17):1007A-1017A. doi:10.1021/ac00144a725
30. Ketterer ME, Reschl JJ, Peters MJ. Multivariate calibration in inductively coupled plasma mass spectrometry. *Anal Chem*. 1989;61(18):2031-2040. doi:10.1021/ac00193a007
31. Watson JT, Sparkman OD. *Introduction to Mass Spectrometry: Instrumentation, Applications and Strategies for Data Interpretation*. 4thed. John Wiley & Sons; 2007. doi:10.1002/9780470516898
32. Hiden Analytical Limited. Training Materials, provided by Hiden Analytical in the training course in the IFP Energies Nouvelles, Technical specifications, Rueil-Malmaison. 2020.
33. International Union of Pure and Applied Chemistry. Nomenclature, symbols, units and their usage in spectrochemical analysis. II. Data interpretation. *Anal Chem*. 1976;48:2294-2296.
34. Long GL, Winefordner JD. Limit of detection. A closer look at the IUPAC definition. *Anal Chem*. 1983;55(7):712A-724A. doi:10.1021/ac00258a001

How to cite this article: Keita S, Noirez S, Berthe G, et al. Development of quantitative detection method for mass spectrometry coupled to an infrared laser spectroscope (Picarro) to monitor in nitrogen matrix a complex gas mixture of H_2, He, CO, N_2, Ne, O_2, Ar, CO_2, H_2S, CH_4, C_2H_4, C_2H_6, C_3H_6, C_3H_8, *i*-C_4H_{10}, *n*-C_4H_{10}, and C_5H_{12}. *Rapid Commun Mass Spectrom*. 2023;37(19):e9614. doi:10.1002/rcm.9614